Magnetostrictive torsional strain in transverse-field-annealed Metglas® 2605

M. Liniers, V. Madurga, M. Vázquez, and A. Hernando
Laboratory of Magnetism, Faculty of Physics, Universidad Complutense, 28003 Madrid, Spain
(Received 23 January 1984)

Amorphous metals exhibit excellent magnetomechanical properties and have been considered for transducer applications. We report an experimental study on the magnetostrictive torsional strain induced under the action of a helical magnetic field in transverse-field-annealed amorphous ribbons with a nominal composition of $Fe_{81}B_{13.5}Si_{3.5}C_2$. The torsional deflection reaches large values at about 5 rad m^{-1}. A theoretical model for magnetostrictive torsion is presented. The model is used to obtain direct information about the magnetostriction constant and transverse magnetization process from torsion-angle measurements. Comparison between theory and experiment shows an overall agreement.

I. INTRODUCTION

Amorphous ferromagnetic alloys have been shown to present magnetomechanical properties superior to those of crystalline magnetostrictive samples. It is mainly the lack of anisotropy after suitable heat treatments which allows us to induce very low and homogeneous anisotropies.[1] Several experiments dealing with the field dependence of the resonant frequency for extensional modes have been reported.[2–4] Modzelewski *et al.*[5] found the magnetoelastic coupling coefficient to be 0.98 for annealed ribbons of Metglas® 2605 SC which was the largest value among those previously reported.

Livingston[6] pointed out that twisting or bending could be desirable for some devices. Following this suggestion Hernando and Madurga[7] recently found theoretically that the fractional change of the shear modulus reaches an infinite value by applying a suitable tensile stress in ribbons with a width-wise easy axis. The experiments reported in the same reference[7] were carried out on transverse-field-annealed ribbons of Metglas® 2605 SC from Allied Chemical Corporation. A fractional change of the shear modulus of 50 was experimentally obtained by measuring the resonant frequency of the fundamental torsional mode. Standing torsional waves were excited in a magnetostrictive way.

The purpose of this report is to analyze the fundamental aspects involved in exciting torsional waves. Therefore a study on the torsional strain induced by applying a suitable magnetic field is presented. The experimental arrangement as well as the information about magnetic parameters which can be obtained by measuring the torsion angle are discussed.

It must be pointed out that calculations of the magnetostrictive torsion deflection are complicated in comparing them with the ones required to obtain longitudinal strains. Complications arise from the lack of homogeneity in the applied field producing the twist. Nevertheless the attempt to find a reasonable approximation which yields the relation between the torsion angle and the magnetostriction constant should be desirable. This is due to the large values expected for the magnetostrictive torsion angle, which would drastically reduce the amount of difficulties involved in measuring the magnetostriction constant in a direct way. It is possible to predict the order of magnitude of the expected torsion angle which is roughly given by the shear strain times the inverse of the half thickness. The magnetostrictive shear strain shall be of the same order as the magnetostriction constant, typically 10^{-5}, and the half thickness of the ribbons is about 10^{-5} m. Consequently a few units of rad m^{-1} is expected for the maximum torsion angle which could easily be measured with the more simple device.

The difficulties related to calculation disappear in the case of thin tubes. Direct measurements of the magnetostriction constant were accurately performed by Drosdziok and Wessel in Ni and Mu-metal tubes utilizing the same idea.[8]

II. THEORETICAL BACKGROUND

As is well known, when a direct current is flowing through a magnetostrictive rod and simultaneously an axial magnetic field is applied a twisting of the rod appears. This phenomenon is called the Wiedemann effect.[9] It has recently been used by Savage and Abbundi[10] for measuring the transverse magnetoelastic coupling coefficient, and it is the basis of the experiment reported here.

Torsion in a thin ribbon of thickness $2a$ and width $2b$ produces an inhomogeneous distribution of shearing strains which varies linearly along the thickness (x axis in Fig. 1). If the ribbon is assumed to be infinitely wide, i.e., $b/a \gg 1$ the complicated strain distribution is reduced to a single component:[11]

$$e_{yz} = \xi a x \ , \tag{1}$$

where ξ is the torsion angle per unit length and x is measured in units of the half thickness a. e_{yz} points in opposite directions in the two halves of the ribbon.

It should be possible to induce magnetostrictively a twist by applying magnetic fields which shift the direction of the magnetization into a helical path, producing opposite shear magnetostrictive strain in both halves of the ribbon. The dependence of the torsion angle on the applied field is analyzed along the following three steps.

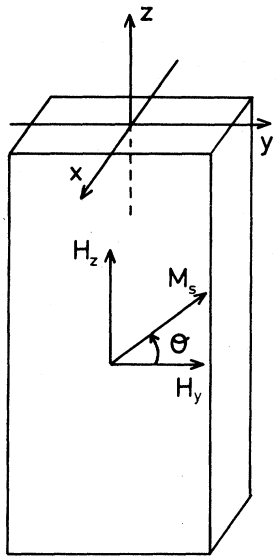

FIG. 1. Schematic view of the geometry of the amorphous ribbon showing the direction of the magnetization M_s, and the applied fields H_z and H_y.

A. Magnetostrictive uniform shear strain

Calculations were restricted to the features corresponding to the samples studied experimentally. The samples were amorphous ribbons with a nominal composition of $Fe_{81}B_{13,5}$ $Si_{3,5}C_2$ obtained from Allied Chemical Corporation (Metlgas® 2605 SC) with 24-μm thickness, 1.6-mm width, and 9-cm length. The ribbons were transverse-field annealed at the Naval Surface Weapons Center, White Oak Laboratory, Maryland, under the following conditions: $t_a=10$ min, $T_a=375\pm2$ °C; the applied magnetic field along the y axis, in Fig. 1, was kept above 1 kOe during the cooling process. This treatment induces a uniaxial anisotropy with the easy axis oriented along the y axis. Typical values of the anisotropy field are close to 0.7 Oe.

We consider a ribbon with a first-order uniaxial anisotropy, with a width-wise magnetic easy axis. We assume a magnetic field H_y is applied along the positive y axis, saturating the sample. When an axial magnetic field H_z is applied the magnetization will rotate an angle θ from width toward the field direction.

Magnetization rotation produces a change in the magnetostrictive strain tensor which can be obtained by minimizing the magnetoelectric and elastic energy densities. The magnetoelastic energy density F_{me} connects the rotation of the magnetization with the strain and, when the magnetization vector is assumed to lie in the ribbon plane, it can be written as follows:[13,12]

$$F_{me}=B(e_{yy}\cos^2\theta+e_{zz}\sin^2\theta+e_{yz}\sin\theta\cos\theta)\ , \tag{2}$$

where the magnetoelastic coupling coefficient B is $B=-3\lambda\mu$, λ is the saturation magnetostriction constant assumed to be isotropic, μ is the shear modulus of the material, and e_{ij} is the magnetostrictive tensor components. The elastic energy term containing the shear-strain components for an isotropic medium is[13]

$$F_{el}=(\mu/2)(e_{xy}^2+e_{yz}^2+e_{xz}^2)\ . \tag{3}$$

Minimization of the total energy density [Zeeman, $F_z=-\mu_0\mathbf{M}_s(\mathbf{H}_y+\mathbf{H}_z)$, anisotropy $F_k=K\sin^2\theta$, magnetoelastic F_{me}, and elastic F_{el} energy densities] with respect to the rotated angle of magnetization θ and components of strain yields, respectively[12] (in absence of any applied stress):

$$K\sin(2\theta)+\mu_0M_sH_y\sin\theta-\mu_0M_sH_z\cos\theta=0\ , \tag{4}$$

$$e_{yz}=\tfrac{3}{2}[\lambda\sin(2\theta)]\ , \tag{5}$$

where K is the anisotropy constant and μ_0M_s the saturation magnetization expressed in teslas. Equation (5) gives through Eq. (4) the relationship between the applied field and e_{yz}.

B. Inhomogeneous shear strain

As shown, the application of a saturating field H_y in conjunction with an axial field H_z results in a pure shear strain. In order to generate a torsional deflection a shear strain increasing with x and opposite in either half of the ribbon must be induced. This can be achieved by making a current I flow through the sample which produces a transverse field $H_y(x)$:[14]

$$H_y(x)=(I/4b)x\ . \tag{6}$$

$H_y(x)$ is opposite in either half of the ribbon. For $I=100$ mA the maximum H_y reached at $x=1$ is 0.4 Oe according to the ribbon width given above.

Since H_y increases linearly with x and changes its direction at $x=0$ the magnetization arrangement shall depend on x. Consequently, exchange interactions must be taken into account. The exchange term is now

$$F_{ex}=\frac{C}{2a^2}\left[\frac{d\theta}{dx}\right]^2\ , \tag{7}$$

where C is the exchange constant.

Minimization of the Zeeman, anisotropy, and exchange energies leads to the following equation for $\theta(x)$:

$$\frac{C}{a^2}\frac{d^2\theta}{dx^2}+\frac{\mu_0M_sI}{4b}x\sin\theta+K\sin(2\theta)-\mu_0M_sH_z\cos\theta=0\ . \tag{8}$$

As a consequence of the symmetry of the problem the magnetization distribution on the $-1<x<0$ part of the ribbon should be the same but inverted with respect to the one corresponding to the $0<x<1$ part. By considering the positive y axis as the origin of rotated angles it should be verified that

$$\theta(-x)=\pi-\theta(x)\ . \tag{9}$$

This condition shows that a kind of wall centered at the plane xy is formed by the effect of I, therefore the adequate boundary conditions for $\theta(x)$ being a solution of Eq. (8) are[15]

$$\theta(0)=\frac{\pi}{2}\ \text{or}\ \frac{3\pi}{2},\quad \theta'(\pm1)=0\ . \tag{10}$$

According to Eqs. (5) and (9), the shear-strain term can be written as

$$e_{yz}(x)=\tfrac{3}{2}\lambda \sin[2\theta(x)]=-e_{yz}(-x)\ , \tag{11}$$

where e_{yz} is opposite in both halves of the ribbon as it is required to induce a twist.

Generally, e_{yz} should not behave linearly along x, therefore the torsion angle per unit length cannot be obtained from Eq. (1). Although different types of approximations can be attempted, the following is preferred. If one assumes that the total elastic energy due to the magnetostrictive strain e_{yz} is employed to generate a pure torsion, then

$$F_{\rm tor}=F_{\rm el}\ , \tag{12}$$

where $F_{\rm tor}$ is the elastic energy per unit area stored along the thickness in a pure torsion which can be calculated from Eqs. (1) and (4),

$$F_{\rm tor}=\frac{\mu}{2}\int_0^1 \xi^2 a^2 x^2 dx\ . \tag{13}$$

$F_{\rm el}$ is the elastic energy stored per unit area along the thickness, originated by magnetostriction, which according to Eq. (4) may be written as

$$F_{\rm el}=\frac{\mu}{2}\int_0^1 e_{yz}^2 dx\ . \tag{14}$$

From Eq. (11) it is finally found that

$$\xi=\frac{\sqrt{3}}{a}\left[\int_0^1 e_{yz}^2 dx\right]^{1/2}\ . \tag{15}$$

We then must find a solution for $\theta(x)$. The influence of the exchange term in Eq. (8) may be analyzed as follows. The uniaxial anisotropy tends to align the magnetization along the y axis, whereas H_y tends to align it along the same axis but in opposite directions on either half. Before applying H_z, minimization of F_k and F_H leads to $\theta(x)=0$ or π for $1>x>0$ and $\theta(x)=\pi$ or 0 for $0>x>-1$, respectively. But such solutions give rise to the appearance of a large exchange energy at $x=0$, where the magnetization presents a shift of 180°. It is known that in order to reduce the exchange energy the inhomogeneity of the magnetization extends along the thickness of the ribbon. The extent of the magnetization inhomogeneities in the vicinity of defects is characterized by the exchange length. At the remanent state, after removing the current, the exchange length is[16] $L_k=(C/K)^{1/2}$ which takes a value of 0.3 μm by taking[17] $C=4\times10^{-11}$ J m^{-1} and $K=60$ J m^{-3}. Then, between $x=0$ and ±0.01, the exchange interaction must be considered to find the magnetization arrangement, but it can be neglected between $x=\pm0.01$ and ±1, where the magnetization is uniform. Since the transverse field is superimposed on the anisotropic one, the exchange length should decrease when some current is flowing through the ribbon. The decreasing rate of L_k as a function of H_y is given by

$$L_k(H_y)=[C/(K+\mu_0 M_s H_y)(x=0.01)]^{1/2}\ . \tag{16}$$

When an axial field H_z is applied the magnetization tends to rotate toward the z axis. Since the rotated angle depends on x, a new source of exchange energy could appear. The maximum θ variation between $x=0$ and 1 is $\pi/2$. By considering that a change of $\pi/2$ requires a $\Delta x=0.01$ to minimize exchange influences, it may be concluded that the magnetization rotation outside the wall, i.e., between $x=\pm0.01$ and ±1, is only governed by the Zeeman and anisotropy energies. In these intervals the exchange term of Eq. (8) can be disregarded. Moreover, the exchange, just as H_z, tends to magnetize the ribbon along the z axis, but for a $H_z=0.1$ Oe the ratio between Zeeman and exchange-energy densities becomes 10^2, consequently the exchange contribution is negligible in comparing it with the H_z contribution.

Figure 2(a) shows the dependence on x of $\sin2\theta$. Curves were numerically calculated from Eq. (8) by neglecting the exchange energy for $H_y(x=1)=1.5$ Oe. However, also shown is a complete solution of Eq. (8) which was obtained by the finite difference method; see Fig. 2(b). Note that only in a small region close to $x=0$ must exchange influences be taken into account.

The torsion angle per unit length as a function of H_z, for $H_y(x=1)=2.5$, 1.5, and 0.75 Oe, is plotted in Fig. 3. Integration indicated by Eq. (15) was numerically performed to obtain these curves.

Calculations predict that ξ reaches a maximum, $\xi_{\rm max}$, for H_z:

$$H_z=(H_y+H_k)0.6\ , \tag{17}$$

where $H_k=2k/\mu_0 M_s$ is the anisotropy field which in this calculation takes a value of 0.7 Oe, K being 60 Jm^{-3} and $\mu_0 M_s=1.7$ T.

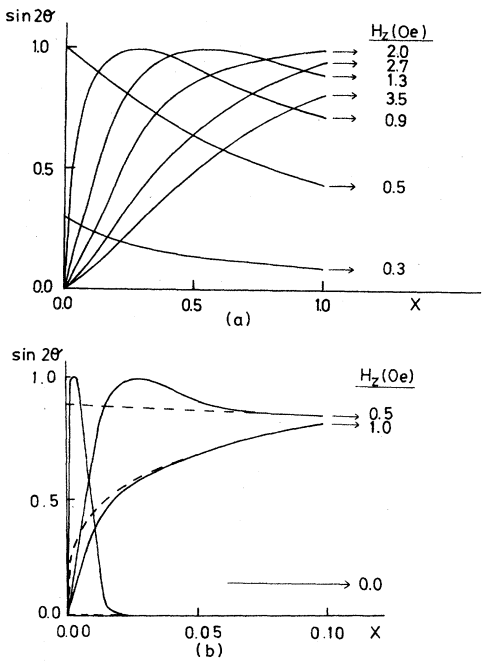

FIG. 2. (a) $\sin2\theta$ as a function of x. Exchange term has been disregarded in Eq. (3). $H_y(x=1)=1.5$ Oe. H_z is the parameter. (b) $\sin2\theta$ as a function of x when the exchange interaction is considered. $H_y(x=1)=0.5$ Oe. Dashed lines indicate the results without considering the exchange term.

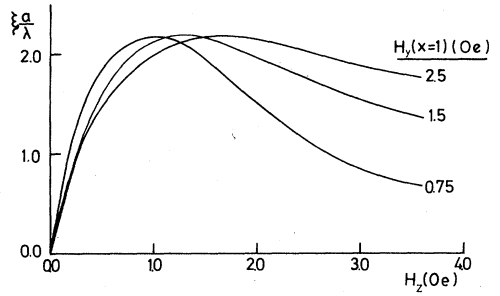

FIG. 3. $\xi a/\lambda$ is shown as a function of H_z. $H_y(x=1)$ is the parameter. These values were obtained by performing the integration given by Eq. (15). e_{yz} was calculated from Eq. (11) by considering the $\sin 2\theta$ values plotted in Fig. 2(a).

ξ_{max} does not depend on H_y and its value is close to $2.2\lambda/a$. It is an important conclusion because the experimental determination of ξ_{max} supply the magnetostriction constant of the ribbon in a direct way.

It must be pointed out that for isotropic samples, i.e., $K=0$ in Eq. (8), an analytical expression for the torsion angle can be found. In this case Eq. (8) yields for $\sin(2\theta)$:

$$\sin(2\theta)=\frac{2H_zH_y(x)}{(H_y^2+H_z^2)^{1/2}} . \tag{18}$$

By substituting Eq. (18) in Eq. (15) through Eq. (11) and after performing the integration, it is found that

$$\xi=\frac{3.6\lambda}{a}\left[\frac{H_z}{H_y}\tan^{-1}\left[\frac{H_y}{H_z}\right]-\frac{H_y^2}{H_y^2+H_z^2}\right]^{1/2} . \tag{19}$$

This dependence is shown in Fig. 4. For the isotropic case, ξ depends on $H_z/H_y(x=1)$ and reaches a $\xi_{max}=2.1\lambda/a$. It is expected that the behavior of relaxed ribbons approximates this model, when the annealing process was performed in the absence of field and stress.

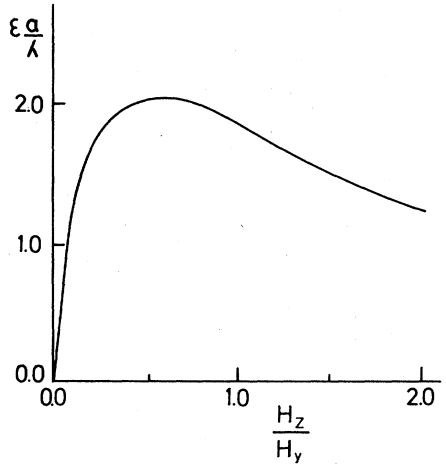

FIG. 4. $\xi a/\lambda$ as a function of $H_z/H_y(x=1)$ for an isotropic ribbon, i.e., $H_k=0$. These points were found from Eq. (19).

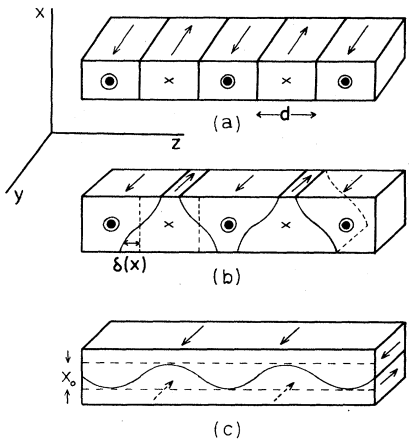

FIG. 5. (a): Typical domain structure as observed for this sample by Livingston (Ref. 18). (b) and (c): Domain-wall motion produced under the effect of an increasing dc current passing through the ribbon.

C. Domain structure and transverse magnetization process

The previous calculations were achieved by assuming the sample to be saturated along the $H_y(x)$ direction in both halves of the ribbon. Actually, the macroscopic transverse magnetization M_y is a function of $H_y(x)$. Several authors have studied the magnetic domain structure of amorphous ribbons exhibiting a width-wise easy axis. Livingston *et al.*[18] observed in transverse-field-annealed Metglas® 2605 SC a domain pattern as shown in Fig. 5. Clearly, in the absence of a dc passing through the ribbon, the sample remains demagnetized along the y axis, thus decreasing the magnetostatic energy. Hsu *et al.*[19] and López *et al.*[20] have analyzed the effect produced on such a magnetic structure by making a current flow along the ribbon. Moreover they found the shape of the walls by minimizing the energy terms involved in the process. Their most important results are summarized in Fig. 5. It can be concluded that a dc current magnetizes a ribbon with a width-wise easy axis by 180° domain-wall motion.

Note that the transverse magnetization must be taken into account to calculate the torsional strain when H_y is not high enough to saturate the ribbon.

As a consequence of the symmetry of the problem, the following discussion will be confined to the $0<x<1$ part of the ribbon, where it is supposed that a transverse field $H_y(x)$ has been applied along the positive y axis.

Let $S^+(x)$ and $S^-(x)$ be the relative areas of domains with magnetization in the same and opposite direction as the field, on the yz sheet of the ribbon placed at x. As is illustrated by Fig. 5,

$$S^+(x)=\frac{1}{2}+\frac{\delta(x)}{d}$$

and (20)

$$S^-(x)=\frac{1}{2}-\frac{\delta(x)}{d} ,$$

where $\delta(x)$ is the mean value of the wall displacement at

x and d is the mean spacing between adjacent walls at the demagnetized state, which according to Livingston[18] is typically of the order of 45 μm.

The reduced macroscopic transverse magnetization in the half thickness becomes

$$m_y=\frac{M_y}{M_s}=\int_0^1 |S^+(x)-S^-(x)|\,dx=\int_0^1 \frac{2\delta(x)}{d}dx \ . \tag{21}$$

If an axial field H_z is applied the magnetization will rotate from width toward the z direction in both kinds of domains, as shown by Fig. 6.

The total shear strain at x should now be

$$e_{yz}(x)=\tfrac{3}{2}\lambda(S^+(x)\sin[2\theta^+(x)] +S^-(x)\sin\{2[\pi+\theta^-(x)]\}) \ , \tag{22}$$

where θ^+ and θ^- are the rotated angles from the initial position corresponding to the magnetization parallel and opposite to H_y. Note that initial position means before applying H_z.

As θ^- is negative, Eq. (22) can be written as

$$e_{yz}(x)=\tfrac{3}{2}\lambda\{S^+(x)\sin[2\theta^+(x)] -S^-(x)\sin[2|\theta^-|(x)]\} \ . \tag{23}$$

In order to evaluate $e_{yz}(x)$ some approximations must be attempted. When the magnetostatic interactions between adjacent domains are neglected, the Stoner-Wohlfarth model[21] predicts that $|\theta^-|$ becomes larger than θ^+ as H_y is increased. If $|\theta^-|$ is larger than θ^+ there will be an effective pole density σ on the wall:

$$\sigma=M_s(\sin|\theta^-|-\sin\theta^+) \ , \tag{24}$$

which will generate demagnetizing fields. Those fields

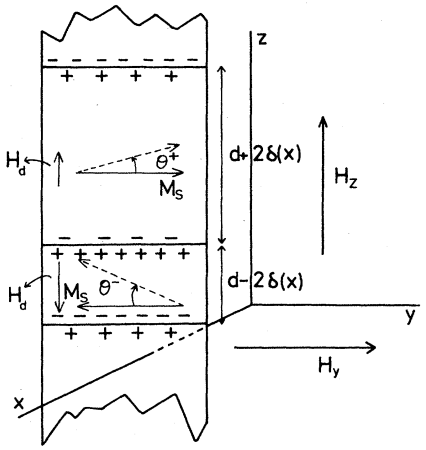

FIG. 6. A yz sheet of the ribbon is shown. H_y acting along the positive y axis produces a domain-wall displacement $\delta(x)$. When H_z is applied, the magnetization tends to rotate different angles for each kind of domain toward the z axis, θ^- being negative. The opposite direction as well as the different strength of the demagnetized fields inside the domains are illustrated.

tend to increase θ^+ and decrease $|\theta^-|$, therefore smoothing the difference expected from the Stoner-Wohlfarth model. The relative strength of both opposite tendencies can approximately be analyzed from the energy terms involved in them. The magnetic fields H_y, H_z, and H_k are typically of the order of 1 Oe whereas, according to the domain dimensions, $2b$, $2a$, and d, the demagnetizing field along the z axis in a domain can approach 0.5 σ. Taking into account the value of M_s given above, it is concluded that in order to obtain comparable energy densities ($\sin|\theta^-|-\sin\theta^+$) must be about 10^{-3}. Consequently no great error would be expected by considering $\theta^+\cong|\theta^-|\cong\theta$.

Note that θ must be between the two values given for θ^+ and $|\theta^-|$ from the Stoner-Wohlfarth model. It can be seen, however, that as a consequence of the domain-wall motion θ should be closer to θ^+. When H_y is low, in comparing it with H_k, the pure rotation model predicts that $\theta^+\simeq|\theta^-|$. As H_y is increased, wall motion increases and the demagnetizing field damping $|\theta^-|$ becomes $(d+2\delta/d-2\delta)$ times θ^+; see Fig. 6. Thus, if we assume that the domain-wall motion occurs, in a substantial amount, for H_y lower than H_K, then θ can be substituted by θ^+. Under this assumption Eq. (23) gives

$$e_{yz}=\tfrac{3}{2}\lambda[S^+(x)-S^-(x)]\sin[2\theta^+(x)] \ , \tag{25}$$

which is an equivalent expression to that given by Eq. (11), both being identical when the transverse saturation has been reached, i.e., $|S^+(x)-S^-(x)|=1$, everywhere. θ^+ is a solution of Eq. (8).

One important implication arising from this formula is that the dc current exerts two different contributions on the shear strain and thus on the torsion angle. The first contribution consists of the transverse magnetizing effect, thus increasing $S^+(x)-S^-(x)$ by domain-wall motion. The second one is related to the torque exerted by H_y on the magnetization which originates the θ^+ dependence on H_y given by Eq. (8).

It is clear from Eq. (25) that the dependence on H_y of $S^+(x)-S^-(x)$ must be known in order to obtain e_{yz} as a function of H_y. As is well established, the wall motion depends on the energy terms involved, which are the magnetostatic energy and the energy coming from the arrangement of defects interacting with walls. Therefore the $S^+(x)-S^-(x)$ dependence on H_y becomes quite difficult to predict. It can be seen, however, that the experiment can elucidate some details of the transverse magnetization process.

The influence of the wall motion on the torsion angle may be analyzed by considering a fixed value of I and assuming different states of the transverse magnetization. For each m_y, a ξ-H_y curve can be calculated as was done at the previous section for $\dot{m}_y=1$.

The numerical integration indicated in Eq. (15) can be performed after determining a suitable dependence on x of $S^+(x)-S^-(x)$. It is to be observed in Fig. 5 that not considering the curvature of the wall, along the thickness of the ribbon, leads to a nearly linear behavior of $S^+(x)-S^-(x)$ with x. With this approximation, two cases must be considered: (a) $\delta(x=1)<d/2$, then $S^+(x)-S^-(x)=[2\delta(x=1)/d]x$; (b) $\delta(x=1)>d/2$, then

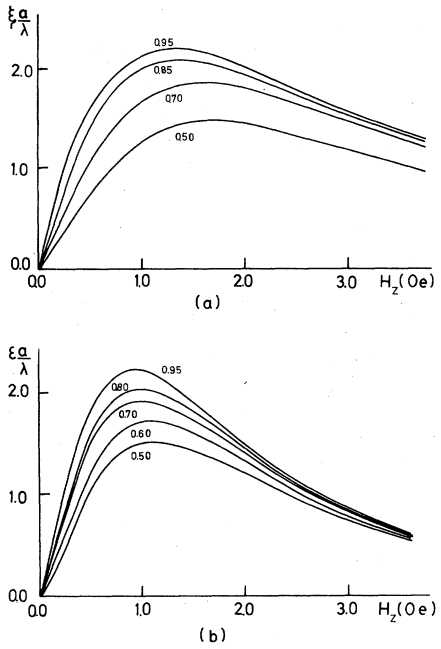

FIG. 7. $\xi a/\lambda$ as a function of H_z for two values of the transversal fields, (a) $H_y(x=1)=1.2$ Oe and (b) $H_y(x=1)=0.6$ Oe. The parameter is m_y. Curves were obtained by considering in Eq. (15) the yz values given from Eq. (25). The relation between $S^+(x)-S^-(x)$ in Eq. (25), which is the parameter, and m_y, is given from Eqs. (20) and (21).

there will be a x_0 satisfying $S^+(x)-S^-(x)=1$ for $x>x_0$ and $S^+(x)-S^-(x)=x/x_0$ for $x<x_0$. According to Eq. (21), m_y should be (a) $m_y=\delta(x=1)/d$, (b) $m_y=1-x_0/2$.

Figure 7 shows the torsion angle per unit length as a function of H_z for a constant I. Two different current values have been considered. Different curves were calculated for different m_y.

ξ_{max} as a function of m_y has been plotted in Fig. 8, where a linear dependence is shown. It is a remarkable result because it means that the experimental determination

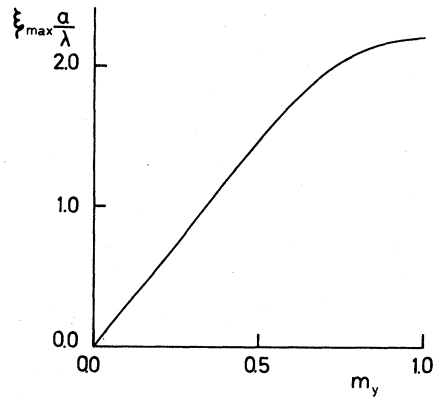

FIG. 8. $\xi_{max}a/\lambda$ as a function of m_y. There is a remarkable linear behavior to allow one to obtain m_y from the ξ_{max} measurements.

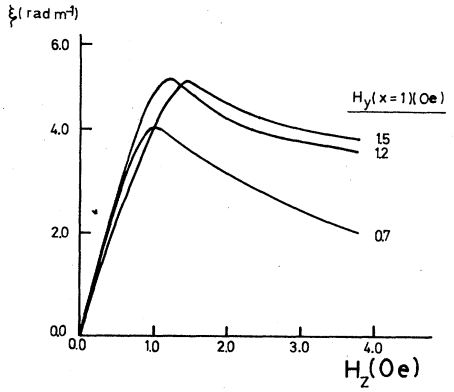

FIG. 9. Experimental ξ-H_z curves are shown for different I values flowing along the ribbon.

of ξ_{max} as a function of I provides direct information about the m_y-H_y magnetization curve.

Finally it is to be expected that for a constant H_z, the dependence on I of ξ_{max} should be quite complex. If $H_z<H_k$, cyclical changes of I will produce hysteresis for ξ as a consequence of the domain-wall motion. The hysteresis should decrease as H_z is increased, and it will vanish for $H_z=H_K$, since in this case the domain structure would be destroyed. It is the superposition of both contributions from I to ξ which yields the complexity of this kind of measurement. Nevertheless, it is easy to see that extrapolation to $H_z=0$ of the coercive force corresponding to the ξ-H_y curves furnishes the coercive force of the m_y-H_y hysteresis loops.

III. EXPERIMENTAL

A. Experimental procedure

The sample was fixed by its upper end to a copper clamp. A thin copper wire 40 μm in diameter was carefully cemented at the lower end of the ribbon by using a conducting silver solution, thus allowing dc current to flow through the sample. The system was placed vertically along the axis of a 25-cm-diam Helmholtz coil. Both coils had an additional winding to compensate for the vertical field of the laboratory. Two dc courses were used to produce the longitudinal (H_z) and transverse (H_y) mag-

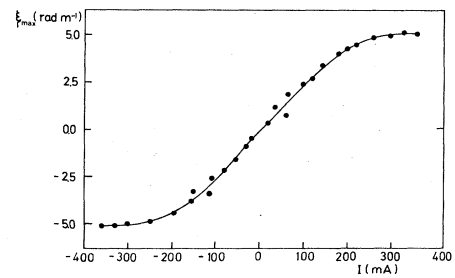

FIG. 10. ξ_{max} as a function of I. The saturation of ξ_{max} reaches a value of 5 rad m^{-1}.

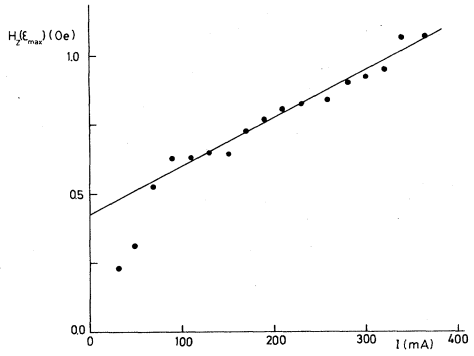

FIG. 11. $H_z(\xi_{max})$ as a function of I.

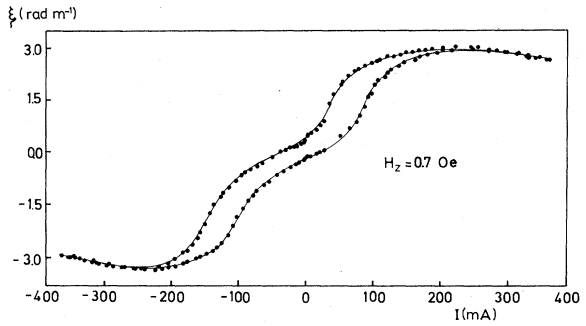

FIG. 12. ξ-I hysteresis loop is shown for H_z constant. $H_z=0.4$ Oe.

netic fields. The current passing through the ribbon never was above 500 mA.

Torsional deflection was measured by using a horizontal laser beam incident on the ribbon 7 cm below the upper end. The reflected spot was displayed on a calibrated screen placed 43 cm from the ribbon. Consequently a 1 mm displacement of the screen spot corresponded to a torsion angle per unit length $\xi=0.03$ rad m^{-1}. Measurements were repeated for different positions of the thin copper wire in order to avoid its possible influence on the ribbon displacement.

B. Experimental results

The torsion angle per unit length was measured as a function of H_z by keeping I constant. The general behavior can be seen in Fig. 9. Cyclical changes of H_z do not produce hysteresis effects. Determination of these curves for different I values provides the ξ_{max} dependence on I which is plotted in Fig. 10. The axial field generating ξ_{max}, $H_z(\xi_{max})$, is a function of I as is illustrated by Fig. 11.

According to the theoretical model developed above the saturation magnetostriction constant as well as the shape of the switching transverse magnetization curve can be inferred from Fig. 10. Since ξ_{max} reaches a saturation value of $2.2\lambda/a$, from its experimental value of 5 rad m^{-1} we obtain $\lambda=2.8\times10^{-5}$, which is in good agreement with the values 2.7×10^{-5} and 3×10^{-5} given by Modzelewski *et al.*[5] and Livingston,[18] respectively, for this sample. The shape of the curve indicates that transverse saturation is approached for $I=200$ mA. As shown by Fig. 11, from $I=200$ mA and for higher values of I the $H_z(\xi_{max})$-I curve has a linear behavior, extrapolation of this straight line to $I=0$ provides H_k through Eq. (17). The value of $H_k=0.66$ Oe is consistent with that given by Modzelewski *et al.*,[5] $H_k=0.7$ Oe. A typical ξ-I hysteresis loop at constant H_z is shown in Fig. 12.

In order to test the suitability of the torsion-angle measurements to find the magnetostriction constant, some experiments were carried out on the glass alloy Metglas® 2826 from Allied Chemical Corp. with nominal composition $Fe_{40}Ni_{40}P_{14}B_6$.

Note that quenched ribbons cannot be studied with the experimental technique reported here. By measuring the torsional deflection in as-cast ribbons, a value of ξ_{max} of 10^{-1} rad m^{-1} was obtained. Since the saturation magnetostriction constant of this alloy is 10^{-5} the surprisingly low value of ξ_{max} only can be explained as a consequence of the lack of transverse magnetization. In other words, the dc current I is not high enough to produce transverse magnetization in the amount required to measure λ. There is a true limitation of the method, imposed by the Joule effect; I cannot be increased indefinitely. Nevertheless, as the stress anisotropy is relaxed, after suitable annealing treatments, the transverse susceptibility is increased, thus allowing the measurement of λ.

ξ_{max} as a function of I is plotted in Fig. 13 for a fully relaxed ribbon of Metglas® 2826. The annealing conditions were $T_a=320$ °C and $t_a=2$ h. Neither stress nor field has been applied during the heat treatment. The value obtained for λ was 1.2×10^{-5} since $a=24$ μm in this ribbon.

IV. CONCLUSIONS

A theoretical basis has been established for understanding the magnetostrictive induction of torsional strains in amorphous ribbons. In this framework, the excitation of magnetoelastic torsional waves, such as those discussed in

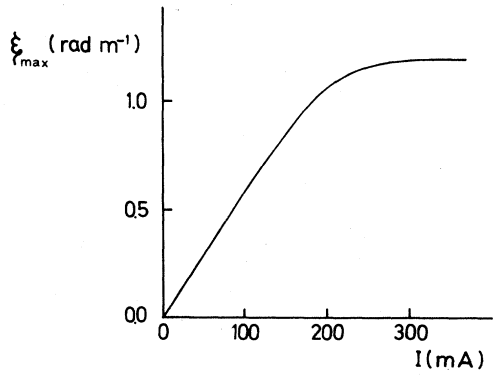

FIG. 13. ξ_{max} as a function of I for a fully relaxed Metglas® 2826 ribbon after annealing 2 h at 320 °C. Saturation of ξ_{max} is 1.3 rad m^{-1}.

Ref. 7, should be explained. Theory predicts and experiment confirms the appearance of large values for the magnetostrictively induced torsional angle. A set of several reasonable approximations leads to direct relations among the experimental data and magnetic parameters: (1) The magnetostriction constant is roughly given by $\lambda = \xi_{max} a/2$, (2) the anisotropy field can be obtained from the extrapolation, at $I=0$, of the $H_z(\xi_{max})$-I lines, and (3) the transverse magnetization curve is obtained from the ξ_{max}-I curve.

Quenched ribbons generally exhibit local anisotropies, originated by microstresses, too high to be transversely magnetized under the action of I. However, ξ_{max} increases for the allowed I values as the structural relaxation is going on. Measurements of ξ_{max} as a function of I, after successive annealing treatments, have been shown to be a quite simple experimental method for monitoring the structural relaxation of amorphous ribbons.

[1]R. N. G. Dalpadado and K. Shirae, J. Appl. Phys. **52(3)**, 1920 (1981).

[2]B. S. Berry and W. C. Pritchet, J. Appl. Phys. **50**, 7594 (1976).

[3]H. S. Chen, Rep. Prog. Phys. **43**, 354 (1980).

[4]A. Hernando, A. García-Escorial, E. Ascasibar, and M. Vázquez, J. Phys. D **16**, 1999 (1983).

[5]C. Modzelewski, H. T. Savage, L. T. Kabakoff, and A. E. Clark, IEEE Trans. Mag. **Mag-17**, 2837 (1981).

[6]J. D. Livingston, Phys. Status Solidi A **70**, 591 (1982).

[7]A. Hernando and V. Madurga, Appl. Phys. Lett. **43**, 799 (1983).

[8]S. Drodsziok and K. Wessel, IEEE Trans. Mag. **Mag-9**, 56 (1973).

[9]H. A. Pidgeon, Phys. Rev. **13**, 209 (1919).

[10]H. T. Savage and R. Abbundi, IEEE Trans. Mag. **Mag-14**, 545 (1978).

[11]A. Hernando and J. M. Barandiarán, Phys. Rev. B **22**, 2445 (1980).

[12]A. Hernando, V. Madurga, and M. Liniers, An. Física **A79**, 136 (1983).

[13]A. Herpin, *Theorie du Magnetisme* (Université de France, Paris, 1968), pp. 381 and 371.

[14]O. V. Nielsen, J. Magn. Magn. Mater. **24**, 81 (1981).

[15]L. Goursat, *A Course in Mathematical Analysis* (Dover, New York, 1964), Vol. III, part 2, p. 253.

[16]H. Traüble, in *Magnetism and Metallurgy,* edited by A. E. Berkowitz and E. Kneller (Academic, New York, 1969), part II, p. 643.

[17]A. Hernando, J. M. Barandiarán, V. Madurga, M. Vázquez, and E. Ascasibar, J. Magn. Magn. Mater. **15—18**, 1537 (1980).

[18]J. D. Livingston, W. G. Morris, and F. E. Luborsky, J. Appl. Phys. **53(11)**, 7837 (1982).

[19]Y. H. Hsu and L. Berger, J. Appl. Phys. **53**, 7873 (1982).

[20]E. López, C. Aroca, and P. Sánchez, J. Magn. Magn. Mater. **36**, 175 (1983).

[21]D. J. Craik, *Structure and Properties of Magnetic Materials* (Pion Limited, London, 1971), p. 139.